Environmental Science and Pollution Research (2021) 28:3972–3982
https://doi.org/10.1007/s11356-020-11834-5

RECENT TRENDS IN ENVIRONMENT AND SUSTAINABLE DEVELOPMENT

A rapid green synthesis of Ag/AgCl-NC photocatalyst for environmental applications

Priyanka Panchal[1] · Poonam Meena[2] · Satya Pal Nehra[1]

Received: 23 February 2020 / Accepted: 23 November 2020 / Published online: 4 January 2021

Abstract

The present study focuses on extract-mediated Ag nanoparticles (NPs), AgCl-NPs, and Ag/AgCl nanocomposites (NCs) as photocatalysts along with its antimicrobial and dye degradation activities. The synthesis of these NPs and NCs was performed by using *Azadirachta indica* plant fruit extract and analyzed using UV-Vis spectroscopy to confirm the synthesis and band gap of these NPs and NCs, X-ray diffraction (XRD) to determine its size and crystalline nature. Fourier transform infrared spectroscopy (FTIR) to discern phytochemicals, responsible for the reduction and capping of the synthesized NCs. Scanning electron microscopy analysis (SEM), transmission electron microscopy analysis (TEM), and energy dispersive X-ray (EDX) spectroscopy analysis were performed to validate the morphology and presence of silver and chloride percentage in the composites. Later, these NPs and NCs were used for their potential role in photocatalytic degradation of methylene blue dye and antibacterial activity against *Escherichia coli* and *Staphylococcus aureus* of human pathogen. The prepared Ag/AgCl-NCs exhibited an enhanced photocatalytic and antibacterial activities in comparison with pure Ag and AgCl nanomaterials. However, green-synthesized NPs and NCs played dual roles as a photocatalyst and antibacterial agent in various biomedical and industrial sectors. Moreover, we found that it might be a hot research in many other environmental applications in upcoming days.

Keywords Green synthesis · *Azadirachta indica* · Nanomaterials · Antibacterial activity · Dye degradation

Introduction

Undoubtedly, semiconductor photocatalyst plays an important role with a good potential for different environmental applications that include mineralization of organic pollutants, water disinfection, hydrogen storage, sensors, photoelectric and biomedical, etc. (Alivisatos 1996; Hoffmann et al. 1995; Khan et al. 2016; Khorrami et al. 2019; Saravanan et al. 2015). Water contamination has been a huge problem in recent years, only 10% of the contaminated water gets purified, and the remaining contaminated water gets released into water bodies as such. If any action not taken, current water supply will decrease by one-third within a couple of decades (Sushmaand Richa 2015; William and William 2015; Ye et al. 2019). Pollutants that are released from home, commercial, industries, and agricultural practices are the key sources of water pollution resulting to organic, inorganic, pathogenic, and non-pathogenic microorganisms, which leads to water-borne pathogens such as protozoan, cholera, intestinal flu, and respiratory infectious agents; these are then transmitted by the fecal-oral route. As drinking water is one of the medium for transmission and causes problems to health and can even lead to death (Cui et al. 2017; Theron and Cloete 2002; Sun et al. 2019), according to the WHO, each year, about 2.2 million populace dies due to diarrhea in which 90% are children, especially in developing countries. For curbing these issues, we are required to provide safe water to everyone (Cui et al. 2017; WHO guidelines 2011; Jin et al. 2014).

Here, the appearance of color in water release from different industries and other areas are also huge issue for the environment as this effluent waste contains heavy metals, organic toxins, lubricants, nutrients, dye solids, chemicals, nutrients from crop fields, house waste, hospital waste, etc. (Bhatia et al. 2017; Gupta et al. 2015; Moradia et al. 2020; Padhi 2012). As textile industries consume dyes that are generally

Responsible Editor: Sami Rtimi

✉ Satya Pal Nehra
nehrasp@gmail.com

[1] Center of Excellence for Energy and Environmental Studies, Deenbandhu Chhotu Ram University of Science and Technology, Murthal 131039, India

[2] Department of Botany, University of Rajasthan, Jaipur 302004, India

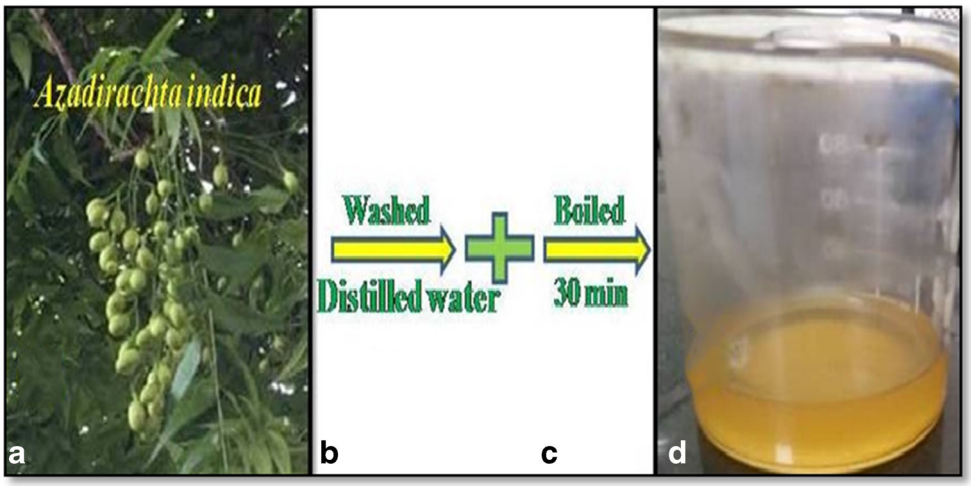

Fig. 1 Plant extract process

in the concentration range of about 10–200 mg L^{-1} and approximately more than 10–15% dyes from the textile, paper, carpet, leather, distillery, and printing industries are released into natural streams and rivers, this creates severe problems as their color stops the progress of re-oxygenation in water by cutting off the dissemination of sunlight. This can lead to the environmental changes and the disruption to the natural balance of the ecosystem (Ashbolt 2004; Araújo et al. 2018; Hongyuan et al. 2019; Páez et al. 2018; Ye et al. 2019; Paul and Nehra 2020). So, it is the responsibility of every person from their respective field to contribute to improve water quality in all possible manners. As new diseases get developed regularly, if we do not get solution on time for older disease, newer one gets to generate and easy to break our immune system. Corona virus (COVID-19) is that type of disease which is generally proving deadly on people already infected with medical problems like cardiovascular, respiratory infection, etc. and you know that most of diseases occur due to direct/indirect use of contaminated water (Guan et al. 2020; Shanmugana et al. 2020; WHO guidelines 2020).

To overcome this major problem, various physical, chemical, and biological methods have been used to investigate the semiconductor photocatalyst. However, these physical and chemical methods require multi-step processing and might prove toxic to the environment (Kumari and Singh 2016; Jamdagni et al. 2018; Malik et al. 2014). Thus, there is a requirement for developing a procedure which will be able to achieve the synthesis of an innovative photo-catalyst in nano-structured form for removal of contamination from waste water (Alishah et al. 2016; Pattanayak et al. 2015; Rashidi and Islami 2020; Saad et al. 2017). In recent years, medicinal plant extract-mediated green synthesis of semiconductor-based photocatalyst gained more attention due to their eco-friendly nature and cost effectiveness. It acts as a reducing and stabilizing agent, and there is no requirement of special areas of synthesis as well. Moreover, plants give a more desirable platform for the synthesis of nanoparticles and are claimed to acquire profit such as their broad variety of natural phytochemicals present in plant extract alkaloids, terpenoids, phenols, flavonoids, tannins, and quinines, etc.; they are free from toxicant chemical. Furthermore, as associate simply offered, safe to use (Ahmad et al. 2015; Bhatia et al. 2017; Jamdagni et al. 2018; Kumari and Singh 2016; Malik et al. 2014; Stamplecoskie and Scaiano 2012).

Nowadays, surface plasmon resonance (SPR) has gained a lot of attention in the field of photocatalysis to enhance the illuminated light reaction of photocatalysts. Several metals like Ag, Au, and Pd have SPR that overlaps with the solar light (Ge et al. 2011; Jiahui and Verma 2012; Zhou et al. 2012; Zada et al. 2020). Among the various metallic ions, Ag is widely used as inorganic nanoparticles with huge applications, as silver (Ag) is the most appropriate selection during dopant due to its tremendous chemical stability, electronic, and optical properties. When Ag nanoparticles lie on the

Table 1 Summary of used characterization tools

Characterizations	Analysis	Results obtained from the analytical techniques
UV-Vis	NPs formation	Verification for the NPs/NCs production and their stability
FTIR	Optical	Recognition of functional groups and chemical bonding
XRD	Structural	Crystallinity, size, structure
SEM and TEM	Morphology and size	Size, morphology, surface irregularity, and texture
EDX	Elemental	Chemical composition and purity

surface photocatalyst, it can considerably increase the interfacial charge-migration kinetic due to SPR (Malik et al. 2014; Nguyen et al. 2020; Panchal et al. 2019a). In the current study, we have reported that the synthesis of Ag-NPs, AgCl-NPs, and Ag/AgCl-NCs has been shown to possess better photocatalytic as well as antibacterial activity potential as compared with the ionic form of the metal, making them one of the most popular metal nanoparticles to be used in photocatalytic and antibacterial applications.

Experimental procedure

Reagents Silver nitrate and sodium chloride are analytically pure, procured from Merck India and used as it was received without further purification.

Plant extract The *Azadirachta indica* plant fruits were brought from herbal garden of South Point College of Pharmacy. To eliminate dirt and contaminants, collected plant fruits were thoroughly washed with distilled water. Washed plant fruits about 20 g were put in Brosile beaker containing 40 mL distilled water. The color changed from transparent to yellow after heating at room temperature (RT) for 30 min. Then, extract was cooled at RT and filtered with filter paper. Then, the collected extract was kept in the refrigerator for further use. The collected plant extract has been shown in Fig. 1 (Panchal et al. 2019b, 2020; Rashidi and Islami 2020).

Ag-NP synthesis A total of 0.1 mM $AgNO_3$ had been used as precursors for green synthesis of Ag-NPs. The solution of precursors was prepared in 250-mL containers by continuously stirring for 1 h using with a magnetic stirrer at RT. Then, 40 mL distilled water was taken and gradually added 10 mL at a time while continuously stirring. The color changed from white to yellowish brown confirming the initial synthesis of Ag-NPs. Then, resultant solutions were cooled at RT and centrifuged at 4000 rpm for 10 min separating the solid particles and washing with alcohol to remove impurities and then kept in hot air oven for drying at 80 °C/8 h. A black sample in powder form was obtained at the end of the procedure (Panchal et al. 2019b, 2020).

AgCl and Ag-modified AgCl-NC synthesis AgCl-NPs and Ag/AgCl-NCs were synthesized using 0.1 mM silver nitrate dissolved in 40 mL distilled water and container labeled with A. Then, 0.3 mM silver nitrate was added with 40 mL distilled water in container B, with the addition of 10 mL fruit extracts (*Azadirachta indica.*) in both containers A and B. Then, the solution in both the containers was continuously stirred for 1 h at RT. After the completion of stirring period, NaCl (0.1 M) was added to both the containers A and B, respectively, again stirred for 1 h. A color change from white to yellowish gray confirmed the initial synthesis of AgCl-NPs and dark grayish color for Ag/AgCl-NCs. Then, resultant solutions were centrifuged at 4000 rpm for 10 min, separated the solid particles, and washed with alcohol to remove contaminants and then kept in hot air oven for dry at 80 °C/8 h. For AgCl-NPs, light gray color and dark gray color for Ag/AgCl-NCs in powder form were obtained at the end of the procedure (Panchal et al. 2019b, 2020).

Photocatalyst characterizations Ag-NPs, AgCl-NPs, and Ag/AgCl-NCs were characterized by various analytical techniques such as UV-Vis spectrophotometer (Lambda750 model of Perkin Elmer in the range of 300-800 nm range in reflection mode), X-ray diffraction (Bruker D8 Advance equipped with CuKα radiation (1.5406 A°), 2θ = 20°-80°), FTIR (Perkin Elmer FRONTIER (250-8000 cm^{-1}) using the standard KBr disk method), SEM with EDS (EVO LS 10), and TEM (Tecnai 20 G2 300 KV, STWIN). Important techniques used for the characterization of green-synthesized NPs/NCs are summarized in Table 1.

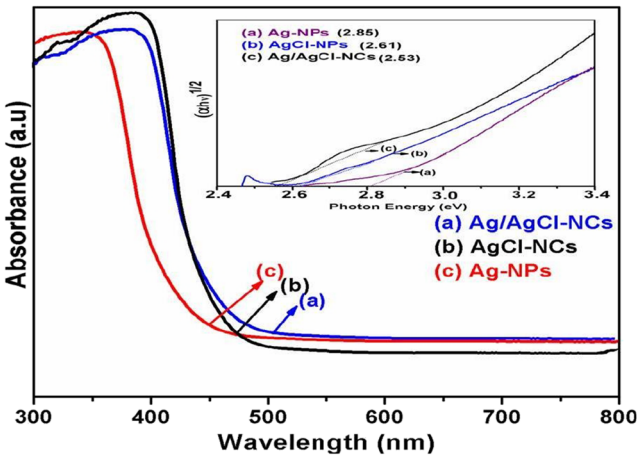

Fig. 2 UV-Vis spectra

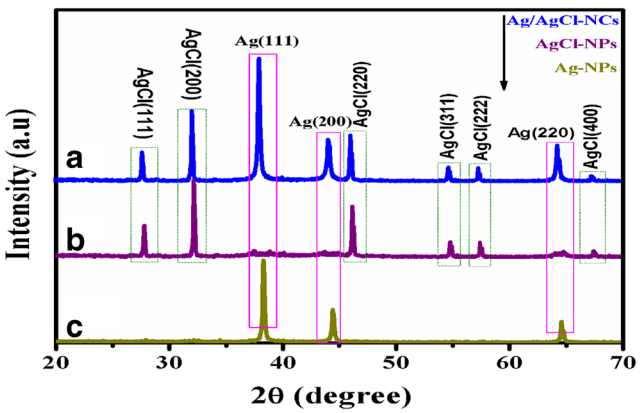

Fig. 3 XRD pattern of a-Ag-NPs, b-AgCl-NPs, c-Ag/AgCl-NCs

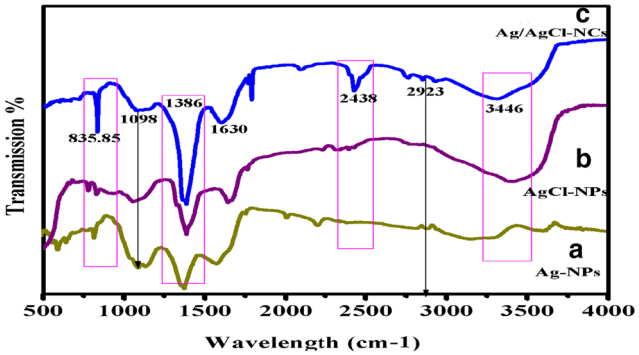

Fig. 4 FTIR spectra of a-pure Ag-NPs, b-AgCl-NPs, and c-Ag/AgCl-NCs

Antibacterial performances Synthesized catalyst was used for antimicrobial activities by a zone of inhibition method. In this experiment, two pathogenic bacteria (s) were used (*E. coli* and *S. aureus*); prior to testing, all glass wares were sterilized in an autoclave for 20 min to make it contamination free. A total of 100-μL bacterial suspension was spread on each sterilized agar media plates (*E. coli* a, b, and c) and (*S. aureus* a, b, and c) spread equally by sterilized spreader. After that, using of sterilized cork borer makes 5 mm diameter well in each plate and added 10-mg catalyst solution of each prepared sample (*E. coli*, a-Ag-Nps, b-AgCl-NPs, and c-Ag/AgCl-NCs and *S. aureus* a-Ag-NPs, b-AgCl-NPs, and c-Ag/AgCl-NCs). Then, plates were left in same condition for 15 min in laminar air flow for proper diffusion of catalyst with agar. Afterward, all plates were kept in an incubator at 37 °C/16 h. After completion of incubation time, plates were removed from the incubator and kept in laminar air flow and zone of inhibition calculated by a metric rule method (Dai et al. 2017; Panchal et al. 2019a, b; Trinh et al. 2015; Villanueva et al. 2015).

Dye degradation performances Methylene Blue (MB) dye decomposition performances were done under direct solar light and confirmed by using UV-Vis spectrophotometer. 10 mg of green-synthesized photocatalysts was added in 100-mL solution having 10 ppm MB dye in three different conical flasks labeled with a-Ag-NPs, b-AgCl-NPs, and c-Ag/AgCl-NC. Prior to exposure under sunlight, all three conical flasks carrying solution of a-Ag-NPs, b-AgCl-NPs, and c-AgCl-NC were stirred without solar light for 30 min to make adsorption-desorption balance of photocatalyst with dye. After that, all samples were kept under solar light irradiation, and at the same time of gap, 5-mL sample was collected and centrifuged to eliminate the solid substances. The decomposition dye solution spectra were recorded using UV-Vis spectrophotometer. The photocatalytic decomposition ability was measured by the following equation: percentage of degradation = $(C_0 - C_t) / C_0 \times 100\%$ (Paul and Nehra 2020; Paul et al. 2019a, b; Panchal et al. 2019b, 2020).

Result and discussion

DRS analysis The UV-visible light DRS were calculated to consider the optical characteristics of Ag-NPs, AgCl-NPs, and Ag/AgCl-NCs as shown in Fig. 2. Prepared samples of Ag/AgCl-NCs are noticeable absorption band edge at 498 nm (Sun et al. 2014), respectively, in evaluation to the absorption edge of Ag-NPs and AgCl-NPs at 482 and 460 nm (Ghosh et al. 2012; Hasan and Asmat 2017). Optical band gap for all samples has been investigated with the equation: $\alpha = A\,(h\nu - E_g)^n / h\nu$, where $\alpha =$ absorption coefficient as shown in the inset of Fig. 2. The energy band gap identified as 2.53, 2.61, and 2.85 eV for Ag/AgCl-NCs, AgCl-NPs, and Ag-NPs, respectively, as shown in the inset of Fig. 2a, b, and c (Wang et al. 2010; Yingying et al. 2018). Ag/AgCl-NCs showed the stronger absorption in direct solar light, due to the maximum metallic Ag nanoparticles present on the surface of Ag/AgCl-NCs which enhance the absorption characteristics of surface plasmon resonance (Jiahui and Verma 2012;Wang et al. 2016; Zhou et al. 2012; Zada et al. 2020). Thus, the increased absorption region of Ag/AgCl-NCs is indicative of favoring the more production of e^-h^+ pairs, which could enhance its photocatalytic activity (Ghosh et al. 2012; Wang et al. 2016; Ye et al. 2012; Yingying et al. 2018).

XRD studies The initial synthesis of Ag-NPs, AgCl-NPs, and Ag/AgCl-NCs can be authenticated by observing the color changed. XRD analyses of Ag-NPs, AgCl-NPs, and Ag/AgCl-NCs were analyzed using X-ray diffractometer. X-ray diffraction peaks were visualized at 2θ value = 38.16°, 44.44°, 64.72°, and 77.52° which corresponded to 111, 200, 220, and 311 which confirmed the synthesis of silver (JCPDS file no 04-0783) as shown in Fig. 3a (Jamdagni et al. 2018; Kumari and Singh 2016). Another six distinct diffraction peaks at 2θ = 28.13°, 32.10°, 46.50°, 55.06°, 57.75°, and 68.16° corresponded to 111, 200, 220, 311, 222, and 400 lattice planes, which confirmed that the synthesis of AgCl-NPs (JCPDS file: 31-1238) can be seen in Fig. 3b (Araújo et al. 2018; Alishah et al. 2016; Panchal et al. 2019a). It can be seen that no Ag peak was noticed here. The reason may be that the quantity of Ag-NPs formed at the surface of the AgCl was low in concentration for detection.

The X-ray diffraction peaks of Ag/AgCl-NCs noticeably showed that the cubic structure of Ag with lattice constant a = 4.0861 A (JCPDS file: 65-2871) similar in the cubic structure of AgCl with lattice constant a = 5.5491 A (JCPDS file: 31-1238) as observed in Fig. 3c (Hasan and Asmat 2017; Sun et al. 2014; Wang et al. 2010). In Ag/AgCl-NCs, increasing the Ag proportion showed different peaks of Ag, whereas that of Cl decreases (Wang et al. 2016). No other peak could be recognized here, which proved the purity of Ag/AgCl-NCs. The sharp and fine diffraction peaks expose the well crystalline nature of particles (Anandalakshmi et al. 2016; Das et al.

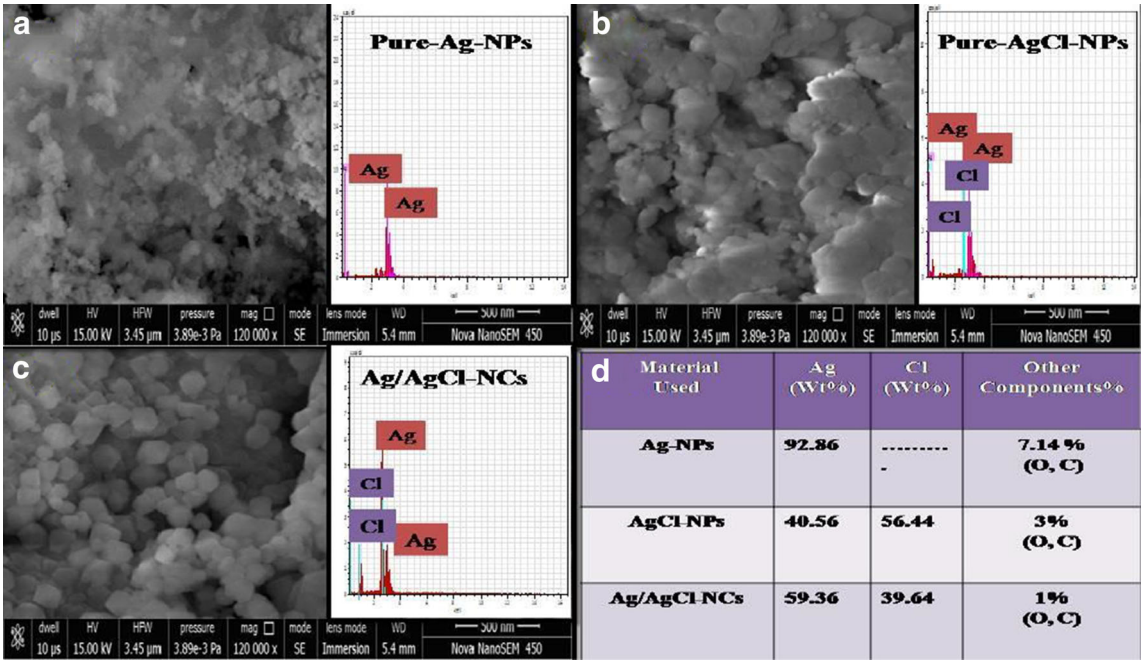

Fig. 5 SEM + EDX studies of a-pure Ag-NPs, b-AgCl-NPs, and c-Ag/AgCl-NCs

2010; Shen et al. 2014; Shaomin et al. 2017; Wang et al. 2016; Ye et al. 2012; Yingying et al. 2018). The crystalline size was observed by Debye-Scherrer's synthesized Ag-NPs, AgCl-NPs, and Ag/AgCl-NCs approximately to 27 nm, 19 nm, and 12 nm.

FTIR studies FTIR studies were used for identification of possible biomolecules present in plant extract which were important for reducing, capping, and stabilization during synthesis of Ag/AgCl-NPs. As shown in Fig. 4, peak appeared at 3446 cm^{-1} which can be recognized to hydrogen bonded O–H functional group of alcohols, phenols, and the occurrence of amines N–H of amide (Anandalakshmi et al. 2016; Shaomin et al. 2017; Wang et al. 2019; Yingying et al. 2018). The –OH is derived from water-soluble phenolic compounds in the plant extract. While the peak vibrations at 2923 cm^{-1} can be attributed to C–H stretching (Anandalakshmi et al. 2016; Wang et al. 2016), the peak at 1630 cm^{-1} is related to a C–OH bond of protein arising from plant extract (Yingying et al. 2018). In the peak at 1386 cm^{-1} related to CO, the peak at 1098 cm^{-1} was recognized to C–O–C bonds in polysaccharides, which are usually found in the region between 1200 and 900 cm^{-1} (Shaomin et al. 2017; Ye et al. 2012). The peak observed at 835.85 cm^{-1} can be approved to the Ag–Cl

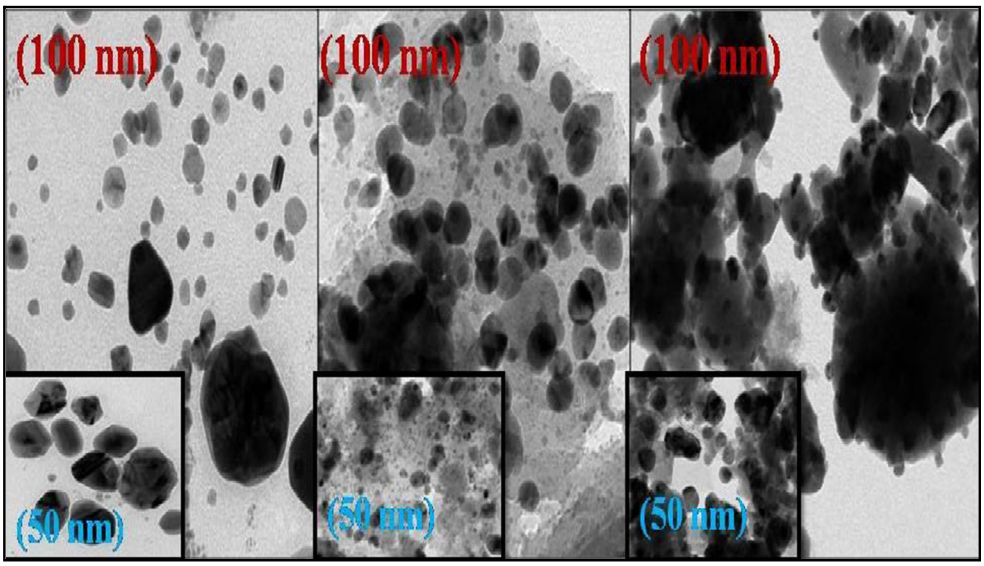

Fig. 6 TEM images of a-Ag-NPs, b-AgCl-NPs, and c-Ag/AgCl-NCs

Table 2 Zone of inhibition towards *E. coli* and *S. aureus*

S.NO	Material	Concentration in mg	Zone of inhibition	
			E. coli	*S. aureus*
1	Ag-NPs	10 mg	10 nm	10 nm
2	AgCl-NPs	10 mg	12 nm	14 nm
3	Ag/AgCl-NCs	10 mg	24 nm	26 nm

stretching vibration. Overall, FTIR data indicated that proteins are key components that drive the bioreduction and stabilization of Ag/AgCl-NCs (Anandalakshmi et al. 2016; Das et al. 2010; Shen et al. 2014; Shaomin et al. 2017; Ye et al. 2012).

SEM and EDX studies Surface morphological study and percentage of elemental composition presented in green-synthesized NPs and NCs were confirmed by SEM and EDX studies. In pure Ag-NPs, a rough aggregated NP surface appeared which may be due to the presence of other elements that may have effects on bioreduction of Ag^{+}; it can be seen in Fig. 5a. After deposition of Cl, it affects the surface morphology of green-synthesized AgCl-NPs, thus decreases the roughness, and little NPs appeared in a closely packed cube-like structure shown in Fig. 5b. In Fig. 5c, Ag/AgCl-NCs appeared bright cubic in shape (Ghosh et al. 2012; Shen et al. 2014; Wang et al. 2010; Yingying et al. 2018). Elemental propagation of the synthesized samples was observed by using EDX analysis that can be seen in Fig. 5d. EDX observation proved the occurrence of used elements: Ag and Cl within the Ag-NPs, AgCl-NPs, and Ag/AgCl-NCs, and table shows the weight percentage in inset of Fig. 5d.

TEM analysis The morphological features of prepared samples were explored using TEM analysis. Metallic Ag-NPs can be observed at the surface of Ag/AgCl-NCs with the clear formation of cubic shape NCs with 10 to 15 nm in size. Two different particles can be seen in Fig. 6c, one is small in spherical and other large in cubic shape. The presented images confirmed that Ag-NPs are spherical in shape with 22 to 30 nm in size as shown in Fig. 6a and AgCl-NPs are in cubic shape with 18 to 20 nm in size as seen in Fig. 6b. Interestingly, the boundaries of AgCl-NCs are decorated through Ag-NPs (Kateryna and Matthias 2018; Zhikun et al. 2014; Jianhua et al. 2019).

Antibacterial studies The antibacterial activities of green-synthesized nanoparticles and nanocomposites were confirmed by the well diffusion method. The pathogenic *E. coli* and *S. aureus* strains were used as a test. A zone of inhibition found during an experimental test is mentioned in Table 2. In presenting work, it was found that bright cubic shape Ag/AgCl-NCs showed highest antibacterial activities in case of *E. coli* and *S. aureus* as compared with pure Ag-NPs and AgCl-NPs as shown in Fig. 7a, b, c. Due to the smaller size, there is a high surface volume ratio and the specific shape of synthesized NCs raised more reactive oxygen species having a greater ability to disturb bacterial cell membrane and directly effect the bacterial metabolism system. After that, bacteria have no ability to further multiply and nanoparticles kill the bacteria (Knuuti et al. 2013; Kabir et al. 2020; Lisdat and Schafer 2008; Nguyen et al. 2020; Panchal et al. 2019b).

Dye decomposition studies Green-synthesized Ag-NPs, AgCl-NPs, and Ag/AgCl-NCs were used here as a photocatalyst towards organic methylene blue dye decomposition. Experimental test performed under direct solar light irradiation and was confirmed by UV-Visible spectrophotometer. It was found that a bright cubic like nanostructured Ag/AgCl-NCs showed the greater degradation efficiency of MB dye in 80 min 92.5%, mainly due to the well and definite

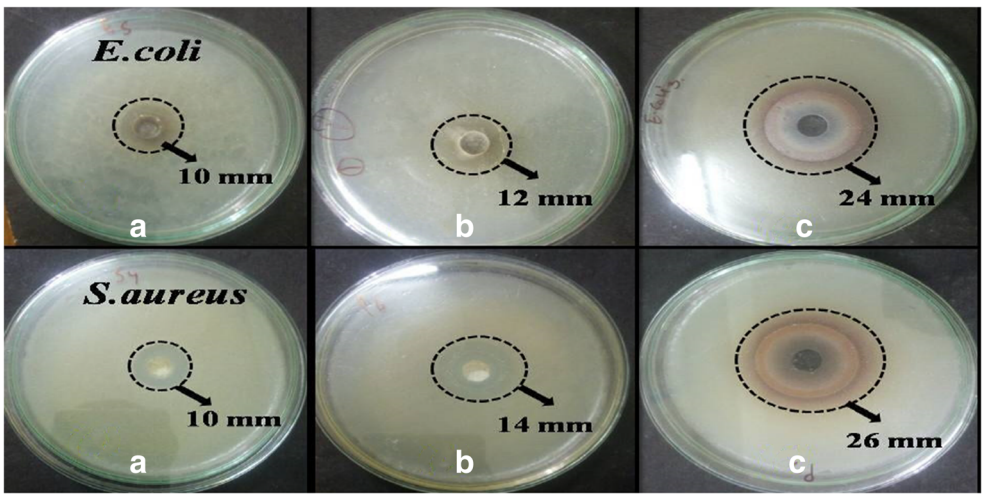

Fig. 7 Antibacterial studies-*E. Coli* (a-pure Ag-NPs, b-AgCl-NPs, and c-Ag/AgCl-NCs) and *S. aureus* (a-pure Ag-NPs, b-AgCl-NPs, and c-Ag/AgCl-NCs)

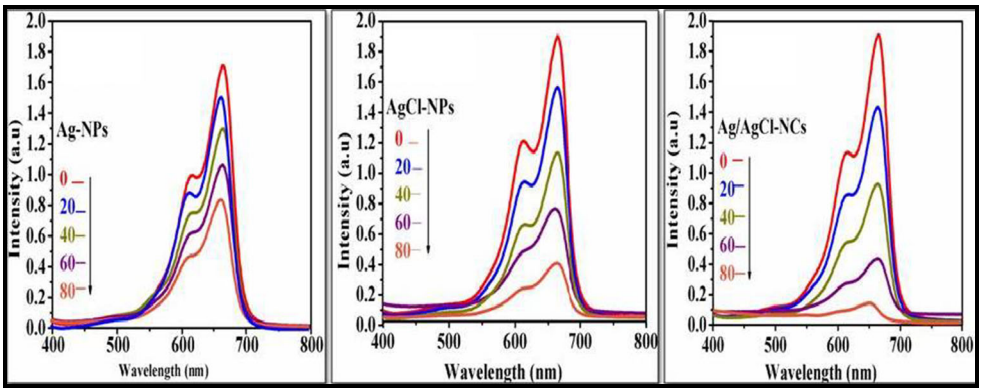

Fig. 8 Dye decomposition studies MB dye spectra of (a-pure Ag-NPs, b-AgCl-NPs, and c-Ag/AgCl-NCs)

morphology can be seen in Fig. 8c as compared with pure Ag-NPs 77.44% and AgCl-NPs 51.46% in 80 min as shown in Fig. 8a, b. For all samples, MB dye decomposition efficiency, dye decomposition percentage, and apparent rate constant were calculated for a time period of about 80 min and have been compared as shown in Fig. 9a, b, c (Araújo et al. 2018; Dai et al. 2017; Rashidi and Islami 2020).

Mechanism Antibacterial inactivation and dye decomposition activities totally depend on synthesized nanostructures' size, morphology, crystalline nature, and band gap (Paul and Nehra 2020; Paul et al. 2019a, b; Rashidi and Islami 2020).

In antibacterial case Bacterial inactivation generally occurred by breaking the cell wall which inhibit the bacterial metabolism system due to which bacteria do not have the capacity to perform any other synthesis like proteins or nucleic acid, which makes changes in membrane permittivity and enzyme formations (Anandalakshmi et al. 2016; Ghosh et al. 2012; Panchal et al. 2019a, b). In this work, synthesized NPs and NCs produce reactive oxygen species (ROS) in the presence of dissolved oxygen, leading to production of large number free radical (Panchal et al. 2020). Then, ROS create disturbances in cell membrane due to bacterial internal cell function and formation like (DNA, mitochondria, lipid, protein

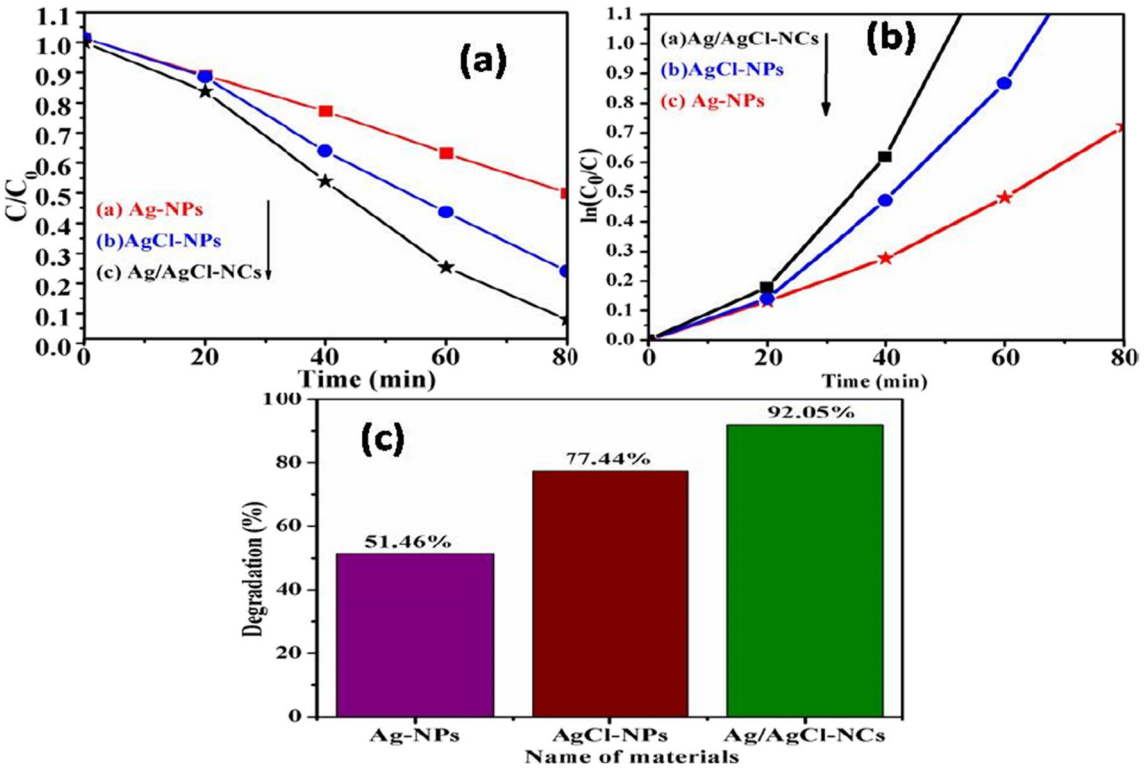

Fig. 9 Dye degradation comparison studies MB **a** degradation spectra, **b** in ($C_0/C(t)$) for dye degradation as function of solar light irradiation time, **c** dye decomposition percentage

Table 3 Showing comparison of *E. coli* and *S. aureus* zone of inhibition with earlier reported works with green-synthesized Ag/AgCl composites

Catalyst	Characterizations		Bacteria ZOI (mm)		References
	NPs size(nm)	Shape	*E. coli*	*S. aureus*	
Ag@AgCl	23	Spherical		16	Alishah et al. (2016)
AgCl/Ag	1.2 ± 0.2 μm	Homogenous hybridizing	2 mm ± 0.5	2 mm ± 0.5	Dai et al. (2017)
Ag/AgCl	16	Cubic	9		Kabir et al. (2020)
Ag@AgCl	15.2	spherical	17	15	Nguyen et al. (2020)
Ag@AgCl	10–30	Spherical, oval	12.67 ± 1.15	14.67 ± 0.58	Patil et al. (2017)
AgCl	90	Spherical	9.82	10.64	Trinh et al. (2015)
AgCl/Ag	20	Cubic	17	12	Villanueva et al. (2015)
Ag/AgCl	15–20	Spherical	17.5 ± 0.5	18.5 ± 0.5	Kota et al. (2017)
Ag/AgCl	12–27	Cubic, spherical	24	26	TW

enzymes, etc.). Totally, disturbed bacteria cells are no longer able to multiply and cause death. Here, green-synthesized Ag/AgCl-NCs show highest antibacterial activities towards both bacterial strains (*E. coli* and *S. aureus*) as compared with all green-synthesized samples (Ag-NPs and AgCl-NPs) as shown in Fig. 7 and mentioned in Table 1. Due to specific particle morphology, small size and lower band gap proved by XRS, DRS, TEM analysis (Anandalakshmi et al. 2016; Ghosh et al. 2012; Lisdat and Schafer 2008; Panchal et al. 2020; Shen et al. 2014).

In dye decomposition case Here, Ag/AgCl-NCs showed the excellent dye decomposition efficiency 92.5% in 80 min as shown in Figs. 8c and 9a, b, c as compared with other synthesized NPs as shown in Fig. 8a and Ag-NPs 77.44% and AgCl-NPs = 51.46% shown in Fig. 8b in 80 min. Ag/AgCl-NCs with low band gap 2.53 when comes into contact with illuminated light are activated and attributed to the SPR effect of Ag-NPs then produced electrons, hole pairs. Then, e− might be moved to molecular O_2 to produce $\cdot O_2^-$, and photoinduced h^+ moved to the AgCl surface coincides to the oxidation of Cl^- to Cl^0. Both $\cdot O_2^-$ and Cl^0 can act as ROS to oxidize MB. At the same time, Cl^0 would be reduced to Cl^- again. Consequently, the Ag/AgCl-NCs showed large and stable photocatalytic efficiency for the degradation of MB (Chung et al. 2014; Hayyan et al. 2016; Knuuti et al. 2013; Paul et al. 2019a, b; Panchal et al. 2020; Sakamoto et al. 2009). Ag/AgCl-NCs bacterial inactivation and dye decomposition mechanism are shown in Fig. 10a, b. Antimicrobial activity and photocatalytic potential of green-synthesized Ag/AgCl-NCs against *E. coli*, *Staphylococcus aureus*, and MB dye degradation have been in comparison with previous published work in Tables 3 and 4.

Conclusion

In this work, cubic structure like Ag/AgCl-NCs is successfully synthesized by the use of plant extract. The XRD graph shows the crystalline nature. SEM and TEM morphology showed that spherical shape Ag-NPs properly deposited on the upper surface of Ag/AgCl-NCs. This exhibits huge surface area of Ag/AgCl-NCs and easier partition of e-h+ pairs. Based on the unique structure and size of prepared Ag/AgCl-NCs, they exhibit improved antibacterial as well as photocatalytic activities as compared with Ag-NPs and AgCl-NPs under direct solar light irradiation. This work explores the better antibacterial

Table 4 Evaluation of MB dye degradation with earlier published works

Catalyst	Characterizations			Dye	Degradation % (Min)	References
	B. Gap	NPs size	Shape			
Ag/AgCl	3.8 eV	27.4 ± 7.4 nm	Heterogeneous	MB	76 (180 min)	Araújo et al. (2018)
AgCl/Ag		1.2 ± 0.2 μm	Homogenous Hybridizing	MB	~ 90(240 min)	Dai et al. (2017)
Ag/AgCl		> 40 nm	Spherical	MB	100 (10 min) 5 ppm	Rashidi and Islami (2020)
Ag/AgCl	2.85 eV	12–27 nm	Cubic, spherical	MB	92.5(80 min) 10 ppm	TW

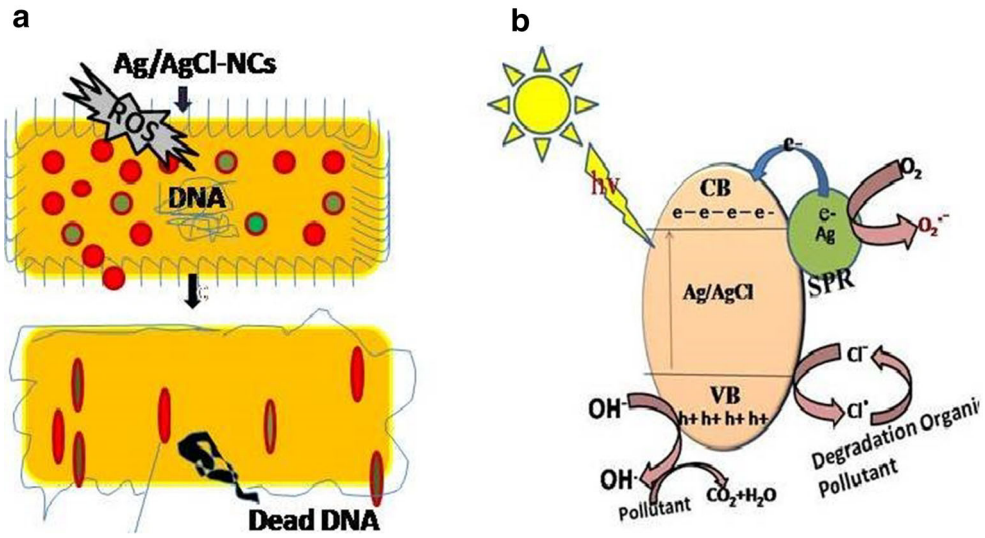

Fig. 10 Proposed mechanism

and photocatalytic performance by good morphology and small size NCs, which could provide not only a simple green method, but also a new approach for designing an effective photocatalyst. Finally, it ought to overcome the restrictions of existing treatment strategies. Moreover, this method will give a secure, solid, and viable treatment towards numerous other environmental applications with excellent efficiency.

Acknowledgments PP is highly thankful to South Point College of Pharmacy, Sonipat for providing antibacterial activity research facilities to do this work. The authors are thankful to Materials Research Center (MRC), Malaviya National Institute of Technology (MNIT), Jaipur for providing characterization facilities.

Authors' contributions P. P. and S. P. Nehra designed the experiment. P. P. and P. M. performed the experiments. P. P. and P.M. analyzed the data. P. P. wrote the draft of manuscript with support from P. M. and S. P. Nehra. S. P. Nehra supervised the project. S. P. Nehra finalized the manuscript.

Funding All India Council for Technical Education, Ministry of Human Resource Development, Govt. of India for provided financial support under Research Promotion Scheme (RPS) reference no. 8-86/RIFD/RPS/POLICY-1/2016-17.

Data availability The data are available upon request.

Compliance with ethical standards

Competing interest The authors declare that they have no competing interest.

Ethical approval For this type of study, formal consent is not required.

References

Ahmad A, Wei Y, Syed F, Imran M, Khan ZUH, Tahir K, Khan AU, Raza M, Khan Q, Yuan Q (2015) Size dependent, catalytic activities of green synthesized gold nanoparticles and electrocatalytic oxidation of catechol on gold nanoparticles modified electrode. RSC Adv. https://doi.org/10.1039/C5RA20096B

Alishah A, Hossein P, Shahram EM, Saeed EM and Ebrahimipou YS (2016) Extract-mediated synthesis of Ag@AgCl nanoparticles using *Conium maculatum* seeds: characterization, antibacterial activity and cytotoxicity effect against MCF-7 cell line RSC Adv 6: 73197–7320210. https://doi.org/10.1039/c6ra16127h

Alivisatos AP (1996) Perspectives on the physical chemistry of semiconductor Nanocrystals. J Phys Chem 100:13226–13239. https://doi.org/10.1021/jp9535506

Anandalakshmi K, Venugobal J, Ramasamy V (2016) Characterization of silver nanoparticles by green synthesis method using Pedalium murex leaf extract and their antibacterial activity. Appl Nanosci 69: 399–408. https://doi.org/10.1007/s13204-015-0449-z

Araújo JN, Tofanello A, Sato JAP, Cruz LS, Nantes-Cardoso IL, Ferreira FF, Batista BL, Garcia W (2018) Rapid synthesis via green route of plasmonic protein-coated silver/silver chloride nanoparticles with controlled contents of metallic silver and application for dye remediation. J Inorg Organomet Polym 28:2812–2818. https://doi.org/10.1007/s10904-018-0947-z

Ashbolt NJ (2004) Microbial contamination of drinking water and disease outcomes in developing regions. Toxicology 198:229–238. https://doi.org/10.1016/j.tox.2004.01.030

Bhatia D, Sharma NR, Singh J, Kanwar RS (2017) Biological methods for textile dye removal from wastewater: a review. Crit Rev Environ Sci Technol 47:1–41. https://doi.org/10.1080/10643389.2017.1393263

Chung D, Khosla A, Gray BL, Parameswaran AM, Ramaseshan R, Kohli K (2014) Investigations of flexible Ag/AgCl nanocomposite polymer electrodes for suitability in tissue electrical impedance scanning (EIS). J Electrochem Soc 161:B3071–B3076

Cui Y, Ma Q, Deng X, Meng Q, Cheng X, Xie M, Li X, Cheng Q, Liu H (2017) Fabrication of Ag-Ag2O/reduced TiO2 nanophotocatalyst and its enhanced visible light driven photocatalytic performance for degradation of diclofenac solution. Appl Catal B Environ 206: 136–145. https://doi.org/10.1016/j.apcatb.2017.01.014

Dai L, Rui L, Li Qiu H, Chuan LS (2017) Simple and green fabrication of AgCl/Ag-cellulose paper with antibacterial and photocatalytic activity. Carbohydr Polym 174:450–455. https://doi.org/10.1016/j.carbpol.2017.06.107

Das R, Nath SS, Chakdar D, Gope G, Bhattacharjee R (2010) Synthesis of silver nanoparticles and their optical properties. J Exp Nanosci 5: 357–362.10.1080/17458080903583915

Ge L, Han C, Liu J, Li Y (2011) Enhanced visible light photocatalytic activity of novel polymeric g-C3N4 loaded with Ag nanoparticles. Appl Catal A 409:215–222. https://doi.org/10.1016/j.apcata.2011.10.006

Ghosh S, Patil S, Ahire M, Kitture R, Kale S, Pardesi K, Cameotra SS, Bellare J, Dhavale DD, Jabgunde A, Chopade BA (2012) Synthesis of silver nanoparticles using *Dioscorea bulbifera* tuber extract and evaluation of its synergistic potential in combination with antimicrobial agents. Int J Nanomedicine 7:483–496. https://doi.org/10.2147/IJN.S24793

Guan WJ, Ni ZY, Hu Y, Liang WH, Ou CQ, He JX (2020) Clinical characteristics of coronavirus disease 2019 in China. N Engl J Med 382:1708–1720. https://doi.org/10.1056/NEJMoa2002032

Gupta VK, Nayak A, Agarwal S (2015) Bioadsorbents for remediation of heavy metals: current status and their future prospects. Environ Eng Res 20:1–18. https://doi.org/10.4491/eer.2015.018

Hasan D, Asmat C (2017) Degradation of blue and red inks by Ag/AgCl photocatalyst under UV light irradiation. AIP Conference Proceedings, 1868:020009. https://doi.org/10.1063/1.4995095

Hayyan M, Hashim MA, AlNashef IM (2016) Superoxide ion: generation and chemical implications. Chem Rev 116:3029–3085. https://doi.org/10.1021/acs.chemrev.5b00407

Hoffmann MR, Martin ST, Choi W, Bahnemann DW (1995) Environmental applications of semiconductor photocatalysis. Chem Rev 95:69–96. https://doi.org/10.1021/cr00033a004

Hongyuan Z, Shangyun L, Xiaomin Z, Hongbo G, Chao M, Chunhui W, Tao D, Qian S, Hu L, Zhanhu G (2019) Super light 3D hierarchical nanocellulose aerogel foam with superior oil adsorption. J Colloid Interface Sci 536:245. https://doi.org/10.1016/j.jcis.2018.10.038

Jamdagni P, Khatri P, Rana JS (2018) Biogenic synthesis of silver nanoparticles from leaf extract of Elettaria cardamomum and their antifungal activity against phytopathogens. Adv Mater Proc 3:129–135. https://doi.org/10.5185/amp.2018/977

Jiahui K, Varma RS (2012) Beet juice-induced green fabrication of plasmonic AgCl/Ag nanoparticles. ChemSusChem 5:1–8. https://doi.org/10.1002/cssc.201200477

Jianhua G, Yuchong C, Jing X, Yujie L, Long Z, Fugeng Z (2019) Fabrication of Ag@AgCl with enhanced plasmonic photocatalysis performance via a deep eutectic solvent. Aust J Chem. https://doi.org/10.1071/CH18386

Jin Y, Liu F, Shan C, Tong M, Hou Y (2014) Efficient bacterial capture with amino acid modified magnetic nanoparticles. Water Res 50:124–134. https://doi.org/10.1016/j.watres.2013.11.045

Kabir SR, Dai Z, Nurujjaman M, Cui X,Asaduzzaman AKM, Sun B, Zhang X, Dai H, Zhao X (2020) Biogenic silver/silver chloride nanoparticles inhibit human glioblastoma stem cells growth in vitro and Ehrlich ascites carcinoma cell growth in vivo. J Cell Mol Med 24:13223–13234. https://doi.org/10.1111/jcmm.15934

Kateryna L, Matthias E (2018) Silver nanoparticles in complex media: an easy procedure to discriminate between metallic silver nanoparticles, reprecipitated silver chloride, and dissolved silver species. RSC Adv 8:24386–24391. https://doi.org/10.1039/c8ra04500c

Khan A, Aslam A, Khan P, Asiri MA, Zied ABM (2016) Green synthesis of thermally stable Ag-rGO-CNT nano composite with high sensing activity. Compos Part B 86:27–35. https://doi.org/10.1016/j.compositesb.2015.09.018

Khorrami S, Abdollahi Z, Eshaghi G, Khosravi A, Bidram E, Zarrabi A (2019) An improved method for fabrication of Ag-GO nanocomposite with controlled anti-cancer and anti-bacterial behavior; a comparative study. Sci Rep 9:9167. https://doi.org/10.1038/s41598-019-45332-7

Knuuti JG, Belevich V, Sharma DA, Bloch, Verkhovskaya M (2013) A single amino acid residue controls ROS production in the respiratory Complex I from *Escherichia coli*. Mol Microbiol 90:1190–1200. https://doi.org/10.1111/mmi.12424

Kota S, Dumpala P, Anantha R et al (2017) Evaluation of therapeutic potential of the silver/silver chloride nanoparticles synthesized with the aqueous leaf extract of Rumex acetosa. Sci Rep 7:11566. https://doi.org/10.1038/s41598-017-11853-2

Kumari J, Singh A (2016) Green synthesis of nanostructured silver particles and their catalytic application in dye degradation. J Genet Eng Biotechnol 14:311–317. https://doi.org/10.1016/j.jgeb.2016.09.005

Lisdat F, Schäfer D (2008) The use of electrochemical impedance spectroscopy for biosensing. Anal Bioanal Chem 391:1555–1567. https://doi.org/10.1007/s00216-008-1970-7

Malik P, Shankar R, Malik V, Sharma N, Mukherjee TK (2014) Green chemistry based benign routes for nanoparticle synthesis. J Nanopart:1–14. https://doi.org/10.1155/2014/302429

Moradia M, Moradia G, Yaghmaeianb K, Yazdanbakhshc A, Srivastavad V, Sillanpäa M (2020) Synthesis of novel Ag-doped S-MgO nanosphere as an efficient UVA/LEDactivated photocatalyst for non-radical oxidation of diclofenac: catalyst preparation and characterization and photocatalytic mechanistic evaluation. Appl Catal B Environ 260:118128. https://doi.org/10.1016/j.apcatb.2019.118128

Nguyen D, Duong N, Nguyen V et al (2020) *Chromolaena odorata* extract as a green agent for the synthesis of Ag@AgCl nanoparticles inactivating bacterial pathogens. Chem Pap 74:1849–1857. https://doi.org/10.1007/s11696-019-01033-z

Padhi BSR (2012) Pollution due to synthetic dyes toxicity & carcinogenicity studies and remediation. Int J Environ Sci 3:3. https://doi.org/10.6088/ijes.2012030133002

Páez C.J., Navío J.A., Hidalgo M.C., Silver-modified ZnO highly UV-photoactive, J Photochem Photobiol, A 356 (2018),112–1122.https://doi.org/10.1016/j.jphotochem.2017.12.044

Panchal P, Malik R, Paul RD, Meena P, Tomer VK, Nehra SP (2019a) Photocatalytic activity of green synthesized AgCl nanoparticles towards *E. coli* bacteria. J Nanosci Nanotechnol 19:1–7. https://doi.org/10.1166/jnn.2019.16839

Panchal P, Paul DR, Sharma A, Hooda D, Yadav R, Meena P, Nehra SP (2019b) Phytoextract mediated ZnO/MgO nanocomposites for photocatalytic and antibacterial activities. J Photochem Photobiol A Chem 385:112049. https://doi.org/10.1016/j.jphotochem.2019.112049

Panchal P, Paula DR, Sharma A, Choudhary P, Meena P, Nehra SP (2020) Biogenic mediated Ag/ZnO nanocomposites for photocatalytic and antibacterial activities towards disinfection of water. J Colloid Interface Sci 563:370–380. https://doi.org/10.1016/j.jcis.2019.12.079

Patil MP, Palma JN, Simeon C, Jin X, Liu X, Ngabire D, Kim N, Tarte H, Kim G (2017) Sasa borealis leaf extract-mediated green synthesis of silver-silver chloride nanoparticles and their antibacterial and anticancer activities. New J Chem 41(3):1363–1371. https://doi.org/10.1039/C6NJ03454C

Pattanayak S, Mollick MMR, Maity D, Chakraborty S, Dash SK, Chattopadhyay S, Roy S, Chattopadhyay D, Chakraborty M (2015) Buteamonosperma bark extract mediated green synthesis of silver nanoparticles: characterization and biomedical applications, In press. https://doi.org/10.1016/j.jscs.2015.11.004

Paul DR, Nehra SP (2020) Graphitic carbon nitride: a sustainable photocatalyst for organic pollutant degradation and antibacterial applications. Environ Sci Pollut Res. https://doi.org/10.1007/s11356-020-09432-6

Paul DR, Sharma R, Panchal P, Malik R, Sharma A, Tomer VK, Nehra SP (2019a) Silver doped graphitic carbon nitride for the enhanced photocatalytic activity towards organic dyes. J Nanosci Nanotechnol (8):5241–5248. https://doi.org/10.1166/jnn.2019.16838

Paul DR, Sharma R, Panchal P, Nehra SP, Gupta AP, Sharma A (2019b) Synthesis, characterization and application of silver doped graphitic carbon nitride as photocatalyst towards visible light photocatalytic hydrogen evolution. Int J Hydrog Energy. https://doi.org/10.1016/j.ijhydene.2019.06.061

Rashidi M, Islami MR (2020) Green synthesis of Ag@AgCl/Elaeagnus angustifolia seed nanocomposite using Elaeagnus angustifolia leaves: an amazing nanophotocatalyst with highly photocatalytic activity under sunlight irradiation. Environ Sci Pollut Res 27: 21455–21467. https://doi.org/10.1007/s11356-020-08598-3

Saad M, Tahir H, Ali D (2017) Green synthesis of Ag-Cr-AC nanocomposites by and its application for the simultaneous removal of binary mixture of dyes by ultrasonicated assisted adsorption process using response surface methodology. Ultrason Sonochem. https://doi.org/10.1016/j.ultsonch.2017.03.022

Sakamoto M, Fujistuka M, Majima T (2009) Light as a construction tool of metal nanoparticles: synthesis and mechanism. J Photochem Photobiol C: Photochem Rev 10:33–56. https://doi.org/10.1016/j.jphotochemrev.2008.11.002

Saravanan RM, Khan M, Gupta VK, Mosquera E, Gracia F, Narayanan V, Stephen A (2015) ZnO/Ag/CdO nanocomposite for visible light-induced photocatalytic degradation of industrial textile effluents. J Colloid Interface Sci 452:126–133. https://doi.org/10.1016/j.jcis.2015.04.035

Shanmugana S, Gorjianb S, Ravichandran S, Panchal H, Essae FA, Kabeelf AE (2020) Global Control Epidemiology of COVID-19: synthesis, characterization and antibacterial screening of silver nanoparticles with *Citrus aurantifolia*. J Xidian Univ 14. https://doi.org/10.37896/jxu14.4/361

Shaomin L, Dinglong Z, Jinglin Z, Qing Y, Huijun W (2017) Preparation of Ag@AgCl-doped TiO2/sepiolite and its photocatalytic mechanism under visible light. J Environ Sci 60:43–52. https://doi.org/10.1016/j.jes.2016.12.026

Shen Y, Chen P, Xiao D, Chen C, Zhu M, Li T, Liu M (2014) Spherical and sheetlike Ag/AgCl nanostructures: interesting photocatalysts with unusual facet-dependent yet substrate-sensitive reactivity. Langmuir 31:602–610. https://doi.org/10.1021/la504328j

Stamplecoskie KG, Scaiano JC (2012) Silver as an example of the applications of photochemistry to the synthesis and uses of nanomaterials. Photochem Photobiol 88:762–768. https://doi.org/10.1111/j.1751-1097.2012.01103.x

Sun L, Zhang R, Wang Y, Chen W (2014) Plasmonic Ag@AgCl nanotubes fabricated from copper nanowires as high performance visible light photocatalyst. ACS Appl Mater Interfaces 6:14819–14826. https://doi.org/10.1021/am503345p

Sun H, Yang Z, Pu Y, Dou W, Wang C, Wang W, Hao X, Chen S, Shao Q, Dong M, Wu S, Ding T, Guo Z (2019) Zinc oxide/vanadium pentoxide heterostructures with enhanced day-night antibacterial activities. J Colloid Interface Sci 547:40–49. https://doi.org/10.1016/j.jcis.2019.03.061

Sushma D, Richa S (2015) Use of nanoparticles in water treatment: a review. Int Res J Environ Sci 4:103–106

Theron J, Cloete TE (2002) Emerging waterborne infections: contributing factors, agents, and detection tools. Crit Rev Microbiol 28:1–26. https://doi.org/10.1080/1040-840291046669

Trinh ND, Nguyen TTB, Nguyen TH (2015) Preparation and characterization of silver chloride nanoparticles as an antibacterial agent. Adv Nat Sci Nanosci Nanotechnol 6:045011. https://doi.org/10.1088/2043-6262/6/4/045011

Villanueva IM, Yañez CMG, Álvarez GR, Hernández PMA, Flores GMA (2015) Aqueous corn husk extract mediated green synthesis of AgCl and Ag nanoparticles. Mater Lett 152:166–169. https://doi.org/10.1016/j.matlet.2015.03.097

Wang P, Huang B, Qin X, Zhang X, Dai Y, Wei J, Whangbo MH (2010) Ag@AgCl: highly efficient and stable photocatalyst active under visible light. Angew Chem Int Ed 47:7931–7933. https://doi.org/10.1002/anie.200802483

Wang H, Lang X, Hao R, Guo L, Li J, Wang L, Han X (2016) Facet defined AgCl nanocrystals with surface-electronic-structure dominated photoreactivities. Nano Energy 19:8–16

Wang H, Lang X, Hao R, Guo L, Li J, Wang L, Han X (2019) Facet-defined AgCl nanocrystals with surface-electronic-structure-dominated photoreactivities. Nano Energy 19:8–16

WHO (2020) Coronavirus disease (COVID-19) Situation Report– 106 Data as received by WHO from national authorities by 10:00 CEST. https://www.who.int/docs/default-source/coronaviruse/situation-reports/20200229-sitrep-40-covid-19.pdf?sfvrsn=849d0665_2. Accessed 5 May 2020

William JC, William PL (2015) Water management: current and future challenges and research directions. Water Resour Res 51:4823–4839. https://doi.org/10.1002/2014WR016869

World Health Organization Guidelines for Drinking-water Quality (2011) Fourth Edition, 564. https://apps.who.int/iris/handle/10665/44584

Ye L, Liu J, Gong C, Tian L, Peng T, Zan L (2012) Two different roles of metallic Ag on Ag/AgX/BiOX(X=Cl,Br) visible light photocatalysts: surface plasmon resonance and Z-scheme bridge. ACS Catal 2:1677–1683. https://doi.org/10.1021/cs300213m

Ye S, Yan M, Tan X, Liang J, Zeng G, Wu H, Song B, Zhou C, Yang Y, Wang H (2019) Facile assembled biochar-based nanocomposite with improved graphitization for efficient photocatalytic activity driven by visible light. Appl Catal B 250:78–88. https://doi.org/10.1016/j.apcatb.2019.03.004

Yingying F, Yu B, Zhongqian S, Zhonghui S, Dandan W, Dongxue H, Li N (2018) Controllable synthesis of coloured Ag^0/AgCl with spectral analysis for photocatalysis. RSC Adv 8:24812–24818. https://doi.org/10.1039/c8ra04180f

Zada A, Muhammad P, Ahmad W, Hussain Z, Ali S, Khan M, Khan Q, Maqbool M (2020) Surface plasmonic-assisted photocatalysis and optoelectronic devices with noble metal nanocrystals: design, synthesis, and applications. Adv Funct Mater 30:1906744. https://doi.org/10.1002/adfm.201906744

Zhikun X, Lei H, Peng H, Shaojun D (2014) Facile synthesis of small Ag@AgCl nanoparticles via a vapor diffusion strategy and their highly efficient visible-light-driven photocatalytic performance. Catal Sci Technol 4:3615–3619. https://doi.org/10.1039/c4cy00889h

Zhou X, Liu G, Yu J, Fanc W (2012) Surface plasmon resonance-mediated photocatalysis by noble metal-based composites under visible light. J Mater Chem 22:21337–21354. https://doi.org/10.1039/C2JM31902K